Competition between Hydrogen Abstraction and Halogen Displacement in the Reaction of Br with CH_3I, CH_3Br, and CH_3Cl†

Karl K. Irikura*

Physical and Chemical Properties Division, National Institute of Standards and Technology, Gaithersburg, Maryland 20899-8380

Joseph S. Francisco

Departments of Chemistry and Earth and Atmospheric Science, Purdue University, West Lafayette, Indiana 47907-2084

Received: February 15, 2007; In Final Form: April 30, 2007

Sudden ozone depletion events in the marine boundary layer are associated with jumps in the CH_3Br mixing ratio, but current models of atmospheric chemistry explain neither the ozone depletion nor the CH_3Br spikes. We have used ab initio theory to predict the forward and reverse rate constants for the competing hydrogen abstraction and homolytic substitution (S_H2) channels of the title reactions. Including the spin−orbit stabilization of the transition structures increases the rate constants by factors between 1.3 and 49. For the atmospherically relevant case of CH_3I, our findings suggest that the hydrogen abstraction and homolytic substitution reactions are competitive. The predicted branching fraction to CH_3Br is about 13%.

Introduction

Bromine species are known to contribute significantly to ozone depletion in much of the stratosphere and in the boundary layer. Measurements since the late 1980s have revealed ozone depletion episodes in the Arctic troposphere during the spring. These dramatic events, in which more than 95% of the ozone disappears within a few hours, are usually attributed to the reactive species Br and BrO.[1−6]

Recent measurements in the arctic boundary layer (below 300 m altitude) have shown an anticorrelation between the concentrations of ozone and of methyl bromide during ozone depletion episodes.[1] Since intact CH_3Br is not believed to catalyze ozone destruction, the spike in its concentration must indicate the presence of a reactive intermediate that was not detected, presumably because it did not survive the sampling and retrieval protocol. Unfortunately, existing models of atmospheric chemistry fail to reproduce the ozone depletion episodes or the observed levels of methyl bromide.[1] Thus, there is an undiscovered source of CH_3Br that involves an ozone-destroying species such as Br or BrO. The authors of the observational study considered a number of possible sources of CH_3Br, both gas phase and heterogeneous. Their best idea was an unknown, low-yield product from reaction between CH_3OO and Br or BrO. They estimated that a rate constant of 2×10^{-14} cm^3 molecule^{-1} s^{-1} for the reaction $Br + CH_3OO \rightarrow CH_3Br + O_2$ would be enough to explain the increased mixing ratio of CH_3Br. However, subsequent ab initio calculations have shown that the reaction between CH_3OO and Br is too slow to be important.[7]

An alternative explanation is exemplified by eq 1. Methyl iodide is the most abundant iodine species in the marine boundary layer,[8,9] although the concentrations measured by Wingenter et al. were low, on the order of 0.3 pptv.[1] The reactions of alkyl iodides with chlorine atoms have been investigated,[10−15] but the analogous reactions with bromine atoms have not been studied. Equation 1 is exothermic, with $\Delta_r H_{298}(1) = -55.9 \pm 0.7$ kJ/mol.[16] If it is fast enough, it can account for the "excess" methyl bromide and will have to be incorporated into atmospheric chemistry models.

$$Br + CH_3I \rightarrow CH_3Br + I \quad (1)$$

$$Br + CH_3\underline{Br} \rightarrow CH_3Br + \underline{Br} \quad (2)$$

$$Br + CH_3Cl \rightarrow CH_3Br + Cl \quad (3)$$

$$Br + CH_3X \rightarrow CH_2X + HBr \quad (4)$$

In this study, eqs 1−3 are examined using well-correlated ab initio computational methods, including effects of spin−orbit coupling, to determine the potential energy profiles and assess whether any of these reactions is a plausible source of CH_3Br. The competing hydrogen abstraction eq 4 is also evaluated to provide estimated branching ratios.

Computational Details[17]

Two basis sets were used for conventional, nonrelativistic calculations of structures, vibrational frequencies, and energetics. The smaller was the 6-31G(d) basis, as defined in the Gaussian03 software package,[18] on all atoms except I, for which it is undefined. The SV4P basis by Andzelm et al. was used on iodine centers.[19] In the aggregate, we refer to this smaller basis set as 6-31G(d) for conciseness, as done previously by Glukhovtsev et al.[20] Cartesian *d*-functions (i.e., 6d) were used in the 6-31G(d) basis set. The larger basis set consists of the 6-311++G(2df,2p) basis on all atoms except I, for which it is also undefined. A corresponding basis for iodine is taken from the work by Glukhovtsev at al., with the *d*-polarization Gaussian exponent split into $\alpha \times 1.5$ and $\alpha/1.5$ as recommended.[20] Contaminants of lower angular momentum were removed from

† Part of the special issue "M. C. Lin Festschrift".

* Corresponding author. E-mail: karl.irikura@nist.gov.

10.1021/jp071314c CCC: $37.00
Published on Web 06/20/2007

the polarization functions (i.e., 5d, 7f) in the 6-311++G(2df,2p) basis set.

The Gaussian03[18] program package was used for all conventional calculations. Vibrational frequencies were computed using numerical differentiation of analytical gradients (QCISD[21]) or double numerical differentiation [QCISD(T)[22]]. In the latter situation, the degeneracy of some vibrations was broken when using the default convergence criteria. Tightening the convergence criteria to 10^{-10} on the SCF density and 10^{-10} on the correlation energy yields acceptably symmetrical results and was done in all QCISD(T) vibrational calculations. Vibrational zero-point energies (ZPEs) were computed as one-half the sum of the harmonic frequencies for the predominant isotopologue. Open-shell calculations were spin-unrestricted. Only valence electrons were included in the correlation treatment. Thermal corrections to the enthalpy were done using the simple rigid-rotor/harmonic-oscillator approximation.[23,24] Vibrational frequencies were not scaled.

Spin contamination in the UHF reference was significant for the S_H2 displacement transition structures, and $\langle S^2 \rangle$ was typically between 0.96 and 1.00 but less than 0.76 after annihilation. To test for convergence in the treatment of electron correlation, geometries were also determined using the CCSD(T)[25] method, which is more complete theoretically than QCISD(T). As an additional test, single-point energies were computed at the well-correlated coupled-cluster BD(TQ)[26] level using the QCISD(T)/6-311++G(2df,2p) geometries. UHF spin contamination was not significant ($\langle S^2 \rangle$ less than 0.79) in the transition structures for eq 4.

Energies from nonrelativistic calculations are spin−orbit averages. Spin−orbit coupling is strong in the halogen atoms, and therefore for all reactions we corrected the calculated atomic energies by amounts derived from experimental energy levels.[27,28] The energy correction is $-E(^2P_{1/2})/3$, or −30.3180, −14.6951, and −3.5184 kJ/mol for I, Br, and Cl atoms, respectively. The experimental levels were also used for computing the atomic partition functions.

Spin−orbit splitting in the open-shell transition structure $[Br\cdots CH_3\cdots I]^‡$ was computed in two ways. The more thorough procedure was a four-component calculation at the relativistic Fock-space coupled-cluster (FSCCSD)[29] level for the ^2A and ^2E states, using an anionic reference, with the program Dirac04.[30] A polarized double-ζ large-component basis set was used (cc-pCVDZ[31] on carbon, cc-VDZ[32] on hydrogen, and uncontracted basis sets by Dyall[33] on the halogens), and the (uncontracted) small-component basis was generated by kinetic balance, for a total of 1058 basis functions. To reduce the cost of the calculation, the interatomic small−small repulsion was modeled classically[34] and only orbitals between −1.5 and +100 hartrees were correlated. The (nonrelativistic) QCISD(T)/6-311++G(2df,2p) geometry was used for the FSCCSD computation.

The less thorough procedure was a full-valence CASSCF(21,15) spin−orbit configuration interaction (SO-CI) mixing the two lowest ^2A and two lowest ^2E states (i.e., six energy eigenvalues) with the program Molpro.[35] Six states were used in the SO-CI to correspond to the three asymptotic states for each halogen atom. An uncontracted polarized double-ζ basis set was used (cc-pVDZ[32] on carbon and hydrogen, small-core Dirac−Fock-optimized pseudopotentials[36] with associated basis sets on halogens). This calculation was done at the same geometry as for the FSCCSD and also (with only three interacting states) at several points along the reaction coordinate,[37] as computed using the hybrid density functional

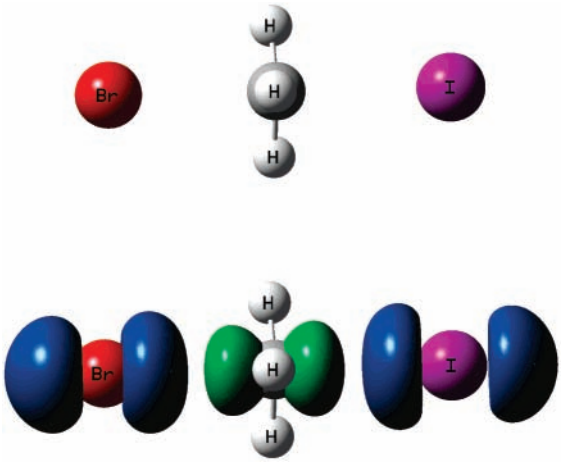

Figure 1. (top) Transition structure and (bottom) UHF spin density (contour of 0.01) for the S_H2 reaction $Br + CH_3I \rightarrow CH_3Br + I$. The point group is C_{3v}.

B3LYP[38−40] with the 6-31G(d) basis set described above. Although the SO-CI calculation is more approximate than the FSCCSD, it has the advantages of greater computational speed and providing an estimate for the ground-state energy lowering due to spin−orbit coupling. For other species, the following numbers of interacting states (from a full-valence CASSCF) were used in the SO-CI to correspond to the asymptotes: three for I and Br, six for IO, BrO, and IBr^+, six for $[Br\cdots CH_3\cdots X]^‡$, and four for $[Br\cdots H\cdots CH_2X]^‡$.

Results

The geometries computed for CH_3X (X = I, Br, Cl) and for the transition structures for eqs 1−3 are summarized in Table 1. Experimental geometries are included for the stable methyl halides. For CH_3Cl, all computed geometries agree with experiment to within 0.006 Å for the bond lengths and within 0.7° for the H−C−Cl bond angle. For CH_3Br, the agreement is within 0.005 Å for the C−H bond length, 0.032 Å for the C−Br bond length, and 0.3° for the H−C−Br angle. The larger basis gives better agreement with experiment (within 0.014 Å for the C−Br distance). For CH_3I, the agreement is within 0.006 Å for the C−H bond length, 0.053 Å for the C−I bond length, and 0.3° for the H−C−I angle. The larger basis again gives better agreement with experiment (within 0.018 Å for the C−I distance). In general, the QCISD(T) and CCSD(T) geometries are almost indistinguishable. The QCISD(T)/6-311++G(2df,2p) geometry for $[Br\cdots CH_3\cdots I]^‡$ and corresponding UHF spin density are illustrated in Figure 1.

The atoms Br−C−X are collinear in the transition structures for eqs 1−3. The point groups of the structures are C_{3v} for X = (I, Cl) and D_{3h} for X = Br. The C−H bond length in the transition structure is similar to that in the reactant methyl halide (0.007 Å shorter). The transition state moves later along the reaction coordinate in the sequence X = I, Br, Cl, as evident from the decreasing Br···C distance (2.37, 2.32, and 2.27 Å, respectively), the increasing Br···C−H angle (88°, 90°, and 92°), and the increasing elongation in the C−X bond (15, 19, and 24%). This trend is consistent with the increasing reaction enthalpy (discussed below). The geometries of the transition structures are more sensitive to the computational details than are those of the methyl halides, but the QCISD(T) and CCSD(T) results are again nearly the same.

The geometries computed for the products and transition structures for eq 4 are summarized in Table 2. For comparison,

TABLE 1: Geometries Relevant for Eqs 1−3[a]

			CH_3X			$[Br\cdots CH_3\cdots X]^{\ddagger}$			
method	basis set	X	r(CH)	r(CX)	θ(HCX)	r(CH)	r(CBr)	r(CX)	θ(BrCH)
QCISD	6-31G(d)	I	1.089	2.180	107.6	1.082	2.405	2.524	87.8
		Br	1.090	1.961	107.7	1.082	2.342	2.342	90.0
		Cl	1.091	1.787	108.8	1.082	2.316	2.238	90.6
	6-311++G(2df,2p)	I	1.083	2.145	108.0	1.076	2.372	2.481	88.3
		Br	1.083	1.941	108.0	1.076	2.321	2.321	90.0
		Cl	1.084	1.786	108.5	1.076	2.274	2.213	91.5
QCISD(T)	6-31G(d)	I	1.090	2.185	107.5	1.084	2.410	2.522	87.5
		Br	1.091	1.965	107.7	1.084	2.344	2.344	90.0
		Cl	1.093	1.790	108.8	1.084	2.314	2.241	90.7
	6-311++G(2df,2p)	I	1.085	2.150	107.9	1.078	2.373	2.472	88.0
		Br	1.085	1.947	107.9	1.078	2.322	2.322	90.0
		Cl	1.086	1.791	108.5	1.078	2.267	2.215	91.7
CCSD(T)	6-311++G(2df,2p)	I	1.085	2.150	107.9	1.078	2.374	2.470	87.9
		Br	1.084	1.946	107.9	1.077	2.320	2.320	90.0
		Cl	1.085	1.790	108.5	1.078	2.267	2.215	91.7
expt (r_0)[64]		I	1.084	2.132	107.7				
		Br	1.086	1.933	107.7				
		Cl	1.090	1.785	108.1				

[a] Distances in Å, angles in degrees.

TABLE 2: Geometries Relevant for Eq 4[a,b]

molecule	r(CX)	r(CH)	θ(HCX)	r(BrH)	φ(HCXH′)	θ(BrHX)
CH_2I	2.051	1.077	118.7			
CH_2Br	1.855	1.076	117.9			
	(1.848)[41]	(1.084)[41]	(117.8[c])[41]			
CH_2Cl	1.711	1.082	118.0			
	(1.691)[42]	(1.09[c])[42]	(118.7)[42]			
HBr				1.421		
				(1.414)[65]		
$[Br\cdots H\cdots CH_2I]^{\ddagger}$	2.066	1.579,1.082	106.2,115.5	1.528	±108.0	142.9
$[Br\cdots H\cdots CH_2Br]^{\ddagger}$	1.867	1.571, 1.081	106.5, 114.8	1.529	±108.2	144.5
$[Br\cdots H\cdots CH_2Cl]^{\ddagger}$	1.715	1.554,1.082	106.9, 114.8	1.535	±108.3	145.0

[a] From QCISD(T)/6-311++G(2df,2p) calculations. [b] Distances in Å, angles in degrees. Experimental values in parentheses. [c] Fixed during the experimental fitting procedure.

the available experimental data are listed in the table between parentheses. However, the structures for CH_2Cl and CH_2Br were experimentally underdetermined; the value of one parameter was merely postulated by the experimentalists during their data analysis. This complication can be avoided by comparing rotational constants directly. For CH_2Br, the experimental constants are 273.77, 11.395, and 10.932 GHz,[41] while the computed values are 277.2, 11.32, and 10.87 GHz. For CH_2Cl, the experimental constants are 274.4, 15.948, and 15.057 GHz,[42] while the computed values are 276.8, 15.80, and 14.95 GHz. Overall, agreement between theory and experiment is acceptable.

Vibrational frequencies were computed to obtain ZPEs and partition functions and to characterize optimized geometries as either minima or first-order saddle points (viz., transition structures). The results are summarized in Table 3 as obtained at the QCISD(T)/6-31G(d) level. For all transition structures, the vibrational mode associated with the imaginary frequency corresponds to the motion expected for the associated reaction. To compute energies at zero temperature, the ZPEs are added to the equilibrium energies listed in Tables 4 and 5. After adding atomic spin−orbit corrections (described above) and the thermal corrections (not tabulated), we obtain reaction enthalpies and enthalpic barriers for eqs 1−4. These are collected in Tables 6 and 7. Experimental reaction enthalpies were computed using the reference data summarized in Table 8.[16]

For the CH_2X radicals, the QCISD(T)/6-31G(d) calculations gave nonplanar equilibrium geometries. With the larger basis set, QCISD(T)/6-311++G(2df,2p), planar geometries were obtained for all three radicals (X = I, Br, and Cl). For these species, the vibrational frequencies and rotational constants in Table 3 were therefore computed using the larger basis set. Rotational spectroscopy indicates that both CH_2Cl and CH_2Br are planar (positive-valued inertial defects).[41,42] In prior computational work, CH_2Br has been predicted to be nonplanar,[43−45] nearly planar,[46−48] and planar.[49] Likewise, previous calculations have found CH_2I to be nearly planar.[50] Thus, the planarity of CH_2X radicals is sensitive to the computational approach; we believe their equilibrium structures are planar but do not investigate this issue further here.

We estimate that our computed reaction enthalpies are reliable to ±5 kJ mol^{-1} (type B standard uncertainty).[51] As shown in Table 6, calculated and experimental values agree when the larger basis set is used. In contrast, the barrier height appears to be more sensitive to the inclusion of perturbative triples (T) than to the choice of basis set. This sensitivity to electron correlation appears to have reached convergence already at the QCISD(T) level; there is negligible change at the slightly more complete CCSD(T) level or even at the fifth-order BD(TQ) level.[26] Thus, we use QCISD(T) for all reaction energetics.

For the competing H-abstraction reaction (eq 4), the results of analogous calculations are collected in Table 7. On the basis of the convergence study for the displacement reactions, we accept the QCISD(T)/6-311++G(2df,2p) results as reliable. Agreement with experimental thermochemistry for eq 4 is not

TABLE 3: Vibrational Frequencies, ZPEs, and Rotational Constants[a]

species	point group	frequencies (cm^{-1})	ZPE (kJ/mol)	rotational constants (cm^{-1})
CH_3I	C_{3v}	a_1: 3115, 1336, 522 e: 3231, 1507, 925	97.5	5.156, 0.241, 0.241
CH_3Br	C_{3v}	a_1: 3109, 1374, 604 e: 3222, 1520, 984	98.9	5.162, 0.312, 0.312
CH_3Cl	C_{3v}	a_1: 3097, 1442, 756 e: 3199, 1523, 1066	100.9	5.212, 0.440, 0.440
$[Br\cdots CH_3\cdots I]^{\ddagger}$	C_{3v}	a_1: 777*i*, 3157, 927, 126 e: 3332, 1436, 984, 117	95.4	4.755, 0.0142, 0.0142
$[Br\cdots CH_3\cdots Br]^{\ddagger}$	D_{3h}	a_1': 3157, 149 a_2'': 853*i*, 958 e′: 3331, 1436, 112 e″: 1012	96.0	4.749, 0.0194, 0.0194
$[Br\cdots CH_3\cdots Cl]^{\ddagger}$	C_{3v}	a_1: 914*i*, 3157, 1000, 189 e: 3329, 1437, 1030, 120	96.8	4.749, 0.0327, 0.0327
HBr	C_v	σ: 2594	15.5	8.115
CH_2I[b]	C_{2v}	a_1: 3185, 1373, 634 b_1: 233; b_2: 3331, 853	57.5	9.356, 0.293, 0.284
CH_2Br[b]	C_{2v}	a_1: 3190, 1396, 711 b_1: 118; b2: 3343, 929	57.9	9.245, 0.378, 0.363
CH_2Cl[b]	C_{2v}	a_1: 3191, 1429, 847 b_1: 140; b_2: 3340, 1002	59.5	9.235, 0.527, 0.499
$[Br\cdots H\cdots CH_2I]^{\ddagger}$	C_s	a′: 636*i*, 3161, 1409, 1144, 794, 627, 452, 48 a″: 3291, 922, 745, 266	76.9	0.508, 0.0187, 0.0181
$[Br\cdots H\cdots CH_2Br]^{\ddagger}$	C_s	a′: 719*i*, 3160, 1428, 1143, 859, 694, 432, 54 a″: 3291, 988, 798, 290	78.6	0.605, 0.0244, 0.0236
$[Br\cdots H\cdots CH_2Cl]^{\ddagger}$	C_s	a′: 795*i*, 3154, 1465, 1155, 866, 792, 479, 73 a″: 3277, 1072, 800, 286	80.3	0.743, 0.0391, 0.0375

[a] Calculated at the QCISD(T)/6-31G(d) level of theory except as noted. [b] Calculated at the QCISD(T)/6-311++G(2df,2p) level.

TABLE 4: Total Equilibrium Energies (hartree) Relevant for Eqs 1−3

	6-31G(d)		6-311++G(2df,2p)			
species	QCISD	QCISD(T)	QCISD	QCISD(T)	CCSD(T)	BD(TQ)//QCISD(T)
I	−6913.12944	−6913.13035	−6916.94675	−6916.95102	−6916.95099	−6916.95153
Br	−2569.96973	−2569.97059	−2572.49969	−2572.50410	−2572.50408	−2572.50455
Cl	−459.56901	−459.57050	−459.65347	−459.65877	−459.65873	−459.65933
CH_3I	−6952.91071	−6952.91676	−6956.79440	−6956.80774	−6956.80756	−6956.80804
CH_3Br	−2609.77126	−2609.77713	−2612.36314	−2612.37657	−2612.37639	−2612.37676
CH_3Cl	−499.38336	−499.38995	−499.53443	−499.54895	−499.54879	−499.54926
$[Br\cdots CH_3\cdots I]^{\ddagger}$	−9522.85641	−9522.86586	−9529.26797	−9529.28976	−9529.28923	−9529.29064
$[Br\cdots CH_3\cdots Br]^{\ddagger}$	−5179.70500	−5179.71445	−5184.82637	−5184.84848	−5184.84793	−5184.84927
$[Br\cdots CH_3\cdots Cl]^{\ddagger}$	−3069.30316	−3069.31347	−3071.98466	−3072.00803	−3072.00746	−3072.00891

TABLE 5: Total Equilibrium Energies (hartree) Relevant for Eq 4[a]

molecule	energy
HBr	−2573.146760
CH_2I	−6956.139269
CH_2Br	−2611.707788
CH_2Cl	−498.881664
$[Br\cdots H\cdots CH_2I]^{\ddagger}$	−9529.286626
$[Br\cdots H\cdots CH_2Br]^{\ddagger}$	−5184.854699
$[Br\cdots H\cdots CH_2Cl]^{\ddagger}$	−3072.027984

[a] Geometry-optimized QCISD(T)/6-311++G(2df,2p).

quite as good as that for the displacement reactions, but is within 7 ± 3 kJ/mol. The discrepancies may reflect difficulties in the present calculations or in the experimental enthalpies of formation of the CH_2X radicals. Experimental thermochemical data are not available for CH_2I, although a hybrid experimental/theoretical enthalpy of formation of 228.0 ± 2.8 kJ mol^{-1} was reported by Seetula[50] (it implies an H-atom abstraction enthalpy of 65.4 ± 2.9 kJ mol^{-1}). For H-abstraction from CH_3I, the reaction barrier is less than the endothermicity (Table 7). This is simply because of the thermal content in $\Delta_r H_{298}$; $\Delta_r H_0 = 58$ kJ/mol, which is less than the barrier (60 kJ/mol) as it should be.

The transition structures for eqs 1−3 are axisymmetric. The electronic ground state has the unpaired electron on-axis (Figure 1); thus, the state designations are $\tilde{X}^2A_1$ for $[Br\cdots CH_3\cdots I]^{\ddagger}$ and $[Br\cdots CH_3\cdots Cl]^{\ddagger}$ and $\tilde{X}^2A_1'$ for the symmetric case $[Br\cdots CH_3\cdots Br]^{\ddagger}$. The degeneracy of the lowest excited state, ^2E (or $^2E'$), is broken by spin−orbit coupling. (In linear notation, ignoring the hydrogenic asymmetry, these states would be called $^2\Sigma_{1/2}$, $^2\Pi_{3/2}$, and $^2\Pi_{1/2}$.) These molecular states must correlate with the $^2P_{3/2}$ and excited $^2P_{1/2}$ levels of the attacking Br atom and the departing halogen atom. Thus, spin−orbit coupling in the transition structure is expected to affect the reaction barrier. The results of calculations of spin−orbit splittings are listed in Table 9. The purpose of Table 9 is to evaluate the reliability of the computational techniques and to verify the correlation between atomic and molecular spin−orbit levels. For the diatomic test species, we used experimental bond lengths: 1.8676 Å for IO,[52] 1.7172 Å for BrO,[52] and 2.235 Å for IBr^+.[53] Except for the difficult halogen monoxides, both theoretical procedures reproduce experimental splittings fairly well. Spin−orbit calculations along the reaction coordinate indicate that the two lowest states of $[Br\cdots CH_3\cdots I]^{\ddagger}$ converge to the ground $^2P_{3/2}$ level of either asymptote. Thus, the reactant atomic levels $^2P_{3/2}(m_J = \pm 1/2)$, $^2P_{3/2}(m_J = \pm 3/2)$, and $^2P_{1/2}(m_J = \pm 1/2)$ correlate with the transition−structure states $^2A_{1,1/2}$, $^2E_{3/2}$, and $^2E_{1/2}$, respectively. The SO-CI calculations indicate that spin−orbit coupling (primarily with the excited $^2E_{1/2}$ state) lowers the

TABLE 6: Energetics (in kJ/mol) for Eqs 1−3, Br + CH_3X → CH_3Br + X, Including Atomic Spin−Orbit Corrections

		X = I		X = Br		X = Cl	
method	basis set	$\Delta_rH_{298.15}$	barrier[a]	$\Delta_rH_{298.15}$	barrier[a]	$\Delta_rH_{298.15}$	barrier[a]
QCISD	6-31G(d)	−68	76	0	106	43	142
	6-311++G(2df,2p)	−56	81	0	107	56	140
QCISD(T)	6-31G(d)	−67	69	0	99	43	134
	6-311++G(2df,2p)	−56	71	0	96	56	129
CCSD(T)	6-311++G(2df,2p)	−56	71	0	97	56	130
BD(TQ)[b]	6-311++G(2df,2p)	−56	70	0	96	56	128
expt		−55.9 ± 0.7		0		54.9 ± 0.8	

[a] Including ZPE but no thermal contributions (i.e., at $T = 0$). [b] At QCISD(T)/6-311++G(2df,2p) geometries.

TABLE 7: Energetics (in kJ/mol) for Eq 4, Br + CH_3X → CH_2X + HBr, Including Atomic Spin−Orbit Corrections

		X = I		X = Br		X = Cl	
method	basis set	$\Delta_rH_{298.15}$	barrier[a]	$\Delta_rH_{298.15}$	barrier	$\Delta_rH_{298.15}$	barrier
QCISD	6-31G(d)	81	88	79	87	72	84
	6-311++G(2df,2p)	63	69	64	71	60	69
QCISD(T)	6-31G(d)	81	84	78	83	71	79
	6-311++G(2df,2p)	61	60	62	63	58	60
expt		N.A.		59.3 ± 2.8		51.0 ± 3.2	

[a] Including ZPE but no thermal contributions (i.e., at $T = 0$).

TABLE 8: Experimental Enthalpies of Formation[16] (kJ/mol)

species	$\Delta_fH^\circ_{298.15}$
I	106.76 ± 0.04
Br	111.87 ± 0.12
Cl	121.302 ± 0.008
CH_3I	14.4 ± 0.5
CH_3Br	−36.4 ± 0.5
CH_3Cl	−81.87 ± 0.60
HBr	−36.29 ± 0.16
CH_2Br	171.1 ± 2.7[45]
CH_2Cl	117.3 ± 3.1[54]
CH_3	146.7 ± 0.3[66]
BrCl	14.79 ± 0.16
Br_2	30.91 ± 0.11
IBr	40.81 ± 0.14

energy of the ground $^2A_{1,1/2}$ state by $\Delta E^\ddagger_{SOC} = 9.7$ kJ mol^{-1} for [Br···CH_3···I]‡, 3.9 kJ mol^{-1} for [Br···CH_3···Br]‡, and 2.0 kJ mol^{-1} for [Br···CH_3···Cl]‡. Analogous calculations for the transition structures of eq 4 indicate spin−orbit stabilization of 0.6 kJ mol^{-1}; the small value is consistent with the asymmetric structures. The values of $\Delta E^\ddagger_{SOC}$ are collected in Table 10.

To compare competing reactions, we calculated rate constants using the simple transition-state theory (TST), eq 5, where k_B, h, R, and T are the Boltzmann constant, the Planck constant, the gas constant, and the temperature, as usual.

$$k_{TST}(T) = (k_BT/hc^\circ)\exp(-\Delta G^\ddagger/RT) \quad (5)$$

The constant $c^\circ = p^\circ/k_BT \approx 2.43 \times 10^{19}$ molecule cm^{-3} is the ideal-gas number density corresponding to the standard-state pressure ($p^\circ = 1$ bar) at 298 K. Ideal-gas entropies S°_{298} were computed for all species in the rigid-rotor/harmonic-oscillator approximation. Entropies and Gibbs energies of activation, $\Delta S^\ddagger$ and $\Delta G^\ddagger$, are compiled in Table 10. The quantities in Table 10 are based upon geometry-optimized QCISD(T)/6-311++G(2df,2p) equilibrium energies with ZPEs and partition functions based upon Table 3. Transition−structure stabilization due to spin−orbit coupling, $\Delta E^\ddagger_{SOC}$, which lowers the barriers, is also listed in Table 10. The barrier correlating with the $m_J = \pm^3/_2$ level of the ground-state Br atom is much higher than that for the $m_J = \pm^1/_2$ level (Table 9, $^2E_{3/2}$ compared with $^2A_{1/2}$). Its contribution to the rate constant is therefore negligible. One might expect that a factor of one-half should be included in the rate constant to reflect this unreactive component. However, it is implicit in the electronic partition functions (ground-state degeneracies), and therefore it should not be included as an additional correction.

The contribution from tunneling is estimated by multiplying the TST rate by the Wigner correction F_{tunnel} (eq 6), where $\nu^\ddagger$ is the imaginary vibrational frequency. The final rate constant is $k(T) = F_{tunnel}k_{TST}(T)$. Values of k and F_{tunnel} are included in Table 10. For comparison with experiment, rate constants for the reverse reactions are also included in the table.

$$F_{tunnel} = 1 + (ih\nu^\ddagger/kT)^2/24 \quad (6)$$

Since our computed barrier heights are probably reliable only to ±5 kJ/mol (standard uncertainty), our computed rate constants at 298 K are probably reliable to a factor of 8. Rate constants for the reverse of eq 4 have been measured by Seetula[45,50,54] and agree with our computed values well within this margin (Table 10).

Discussion

Among eqs 1−3, only eq 1 is exothermic (Table 6). The competing eq 4 is endothermic (Table 7). Thus, for CH_3I the thermochemistry suggests that the bimolecular homolytic substitution (S_H2)[55] reaction will predominate. However, eq 1 has a significant barrier (Table 6), while eq 4 has a barrier only slightly exceeding its endothermicity (Table 7). This is illustrated in Figure 2 for zero temperature.

The gross effect of spin−orbit coupling on eq 1 is also shown in Figure 2; only one-half (the $m_J = ^1/_2$ component) of the ground-state Br $^2P_{3/2}$ is reactive. Classically, this factor may be obtained by reasoning that the odd electron on Br must reside in the p orbital that points toward the CH_3I, so that only one-third of the ^2P term (i.e., one-half of the ground $^2P_{3/2}$ level) will be reactive. However, classical reasoning does not predict the small (9.7 kJ mol^{-1}) spin−orbit stabilization of the transition structure, which increases the room-temperature rate constant by a factor of 49. Similar spin−orbit correlation diagrams have been used to interpret the analogous exchange reaction between Br and HI[56] and also the photoelectron spectra of anions such as $I^-\cdot CH_3I$[57] and $I^-\cdot$HBr.[58] Since the transition structure for eq

TABLE 9: Excitation Energies (cm^{-1}) of Spin−Orbit Levels Computed Using the FSCCSD and SO-CI Procedures[a]

species	level	expt	FSCCSD	SO-CI
I ($^2P_{3/2}$)	$^2P_{1/2}$	7603.15[67]	7343 (−3%)	7250 (−5%)
Br ($^2P_{3/2}$)	$^2P_{1/2}$	3685.24[27]	3695 (0.3%)	3511 (−5%)
IO ($^2\Pi_{3/2}$)	$^2\Pi_{1/2}$	2091 ± 40[68]	1855 (−11%)	1317 (−37%)
BrO ($^2\Pi_{3/2}$)	$^2\Pi_{1/2}$	967.99[69]	846 (−13%)	604 (−38%)
IBr^+ ($^2\Pi_{3/2}$)	$^2\Pi_{1/2}$	4662 ± 2[70]	4570 (−2%)	4532 (−3%)
$[Br\cdots CH_3\cdots I]^‡$ ($^2A_{1,1/2}$)	$^2E_{3/2}$	N.A.	5795	6264
$[Br\cdots CH_3\cdots I]^‡$ ($^2A_{1,1/2}$)	$^2E_{1/2}$	N.A.	8322	8441
$[Br\cdots CH_3\cdots Br]^‡$ ($^2A''_{2,1/2}$)	$^2E'_{3,2}$	N.A.	N.A.	6812
$[Br\cdots CH_3\cdots Br]^‡$ ($^2A''_{2,1/2}$)	$^2E'_{1/2}$	N.A.	N.A.	8857
$[Br\cdots CH_3\cdots Cl]^‡$ ($^2A_{1,1/2}$)	$^2E_{3/2}$	N.A.	N.A.	7408
$[Br\cdots CH_3\cdots Cl]^‡$ ($^2A_{1,1/2}$)	$^2E_{1/2}$	N.A.	N.A.	8364

[a] Ground-state designations and errors relative to experiment are in parentheses. 1 kJ mol^{-1} = 83.59 cm^{-1}.

TABLE 10: Rate Constants (cm^3 $molecule^{-1}$ s^{-1}) and Activation Energetics at 298.15 K

eq	k	$\Delta S^‡_{298}$ (J mol^{-1} K^{-1})	$\Delta G^‡_{298}$ (kJ mol^{-1})	$\Delta E^‡_{SOC}$ (kJ mol^{-1})	F_{tunnel}	$k_{reverse}$ (calcd)	$k_{reverse}$ (expt)
1	5.9×10^{-23}	−103.0	100.1	9.7	1.59	1.3×10^{-32}	N.A.
2	1.2×10^{-28}	−107.0	127.0	3.9	1.71	1.2×10^{-28}	N.A.
3	2.5×10^{-34}	−100.5	157.6	2.0	1.81	1.3×10^{-24}	N.A.
4-I	4.1×10^{-22}	−92.2	85.9	0.6	1.39	3.4×10^{-13}	$(6.6 \pm 0.6) \times 10^{-13}$ [50]
4-Br	1.8×10^{-22}	−92.1	88.0	0.6	1.50	9.1×10^{-14}	$(2.76 \pm 0.15) \times 10^{-13}$ [45]
4-Cl	6.0×10^{-22}	−92.2	85.3	0.6	1.61	5.7×10^{-14}	$(12.8 \pm 0.4) \times 10^{-14}$ [54]

4 is so asymmetric, spin−orbit coupling is quenched and the rate enhancement is only 30%.

The rate constants that we calculate for eqs 1 and 4, at T = 298 K, are $k_1 = 6 \times 10^{-23}$ and $k_4 = 4 \times 10^{-22}$ cm^3 $molecule^{-1}$ s^{-1} (Table 10). Thus, we predict a branching ratio k_1/k_4 of about 0.14. This ratio is uncertain by a factor of 8, as estimated above. The reliability of our computed rate constants can be estimated on the basis of the reverse of eq 4, since those rates have been measured experimentally.[45,50,54] We find good agreement; the theoretical rates are too low by factors of only 2, 3, and 2 for X = I, Br, and Cl, respectively. Earlier rate calculations using more approximate methods also yielded good results for the reverse of eq 4 (Br) (3.4×10^{-13} cm^3 $molecule^{-1}$ s^{-1})[48] and for the similar reaction $CHClBr + HBr \rightarrow CH_2ClBr + Br$.[59,60] Our rate constants for H-abstraction eq 4 (Br and I) compare well with two earlier, more approximate calculations (1.8×10^{-22} and 2.1×10^{-22}, respectively)[45,50] but disagree with another (1.1×10^{-19})[48] for eq 4 (Br). Our discrepancy with the last value corresponds closely (within 1.8 kJ mol^{-1}) to the spin−orbit correction that should be applied to the bromine atom; it is not stated in that report whether the spin−orbit correction was applied. There do not appear to be any rate constants in the literature for eq 4 (Cl) or its reverse.

We did not find any prior studies of eqs 1−3 in the literature. However, the analogous reactions of chlorine and fluorine atoms have been studied. High-pressure rate constants (at T = 283 K) for halogen displacement by fluorine, $F + CH_3X \rightarrow CH_3F + X$, have been measured as $(8 \pm 3) \times 10^{-13}$, $(1.7 \pm 0.3) \times 10^{-13}$, $(3.7 \pm 1.3) \times 10^{-14}$, and 6×10^{-15} cm^3 $molecule^{-1}$ s^{-1} for X = I, Br, Cl, and F.[61] These, and analogous reactions with larger alkyl iodides,[62] were presumed to be S_H2 reactions, with inversion of configuration at carbon. Note that substitution by

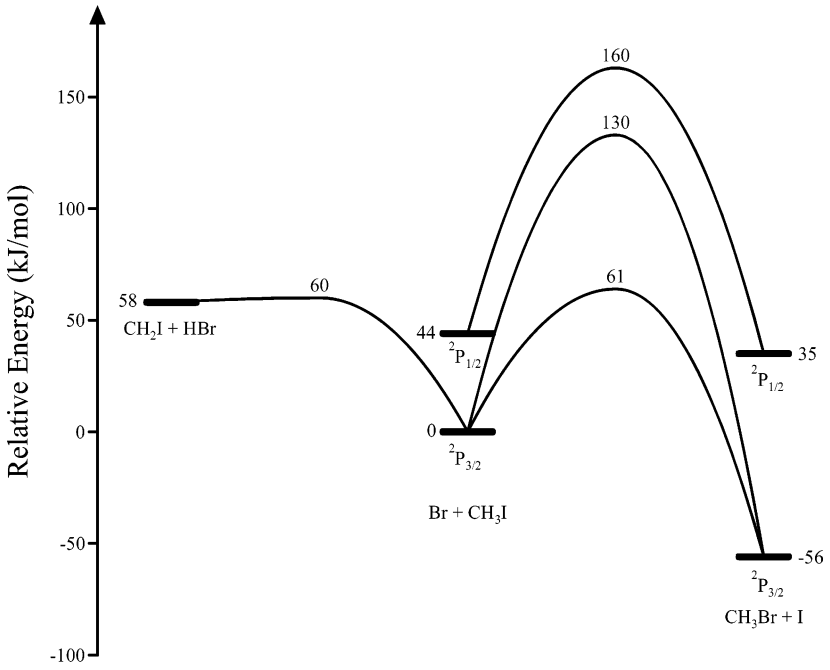

Figure 2. Relative energies (T = 0) for educts and transition structures of eqs 1 and 4.

F is exothermic; for these reactions, we compute (by the same QCISD(T)/6-311++G(2df,2p) procedure described earlier) $\Delta_r H_{298} = -228$, -173, and -117 kJ mol^{-1} for X = I, Br, and Cl.

There have been several studies of the reactions of Cl with alkyl iodides that revealed a more complicated situation. Above 364 K, the main reaction between Cl and CH_3I is H-abstraction as expected, but formation of an adduct, CH_3I-Cl, predominates under typical atmospheric conditions.[11] The CH_3I-Cl bond dissociation enthalpy was determined experimentally to be 52 $\pm$ 3 kJ mol^{-1}, and DFT calculations predicted an acute C−I−Cl bond angle of 85°.[11] The red tail of the visible absorption spectrum of CH_3I-Cl has been recorded.[15] There is substantial charge-transfer character in the bonding, since the strength of the complexation is anticorrelated with the ionization energy of the parent alkyl iodide.[11,15] At 295 K and high pressure, an 8.6% yield of CH_3Cl was observed from Cl + CH_3I at 295 K.[10] Drawing upon unpublished calculations by McGrath and Rowland, both S_H2 and front-side attack (via the adduct) were suggested to be reasonable mechanisms.[10] However, at low pressure no CH_3Cl was detected among the products, ruling out any simple bimolecular origin.[12] Instead, the apparent route to CH_3Cl was effectively termolecular: $CH_3I-Cl + CH_3I \rightarrow CH_3-Cl$ + products.[12] A similar conclusion was reached in a study of ethyl iodide and 2-propyl iodide, although more quantitatively, with upper limits on the direct substitution reactions of 2.5×10^{-12} and 3×10^{-12} cm^3 molecule^{-1} s^{-1}, respectively.[14]

Adducts of the type CH_3X-Br have not been investigated. If bonding is principally due to charge transfer, CH_3I-Br will be more weakly bound than CH_3I-Cl, since the electron affinity of Br (324.5 kJ mol^{-1}) is less than that of Cl (348.7 kJ mol^{-1}).[63] Furthermore, the larger I−Br distance will weaken the ionic bonding. However, some stabilization may be anticipated for a front-side displacement mechanism, which remains unexplored.

Another channel in the reaction Cl + CH_3I, iodine abstraction to yield CH_3 + ICl, has been considered but then dismissed as too endothermic.[13,15] We calculate (as before) $\Delta_r H_{298} = 39$ kJ mol^{-1} for this reaction, modestly endothermic. In contrast, Cl + CH_2ICl yields CH_2Cl + ICl rapidly, $k = 8.5 \times 10^{-11}$ cm^3 molecule^{-1} s^{-1} [12] (calculated $\Delta_r H_{298} = 14$ kJ mol^{-1}), and in the reaction F + CH_3I, the fastest process produces CH_3 + IF[61] (calculated $\Delta_r H_{298} = -22$ kJ mol^{-1}). The analogous process here is eq 7.

$$Br + CH_3X \rightarrow CH_3 + BrX \qquad (7)$$

However, the thermochemistry is unfavorable with bromine: experimentally $\Delta H_{298} = 61.2 \pm 0.6$, 102.1 ± 0.6, and 131.5 ± 0.7 kJ mol^{-1} for X = I, Br, and Cl, respectively (Table 8). For the X = Br case, it has been predicted that the barrier for eq 7 is 38 kJ mol^{-1} higher than that for eq 4.[48] Thus, we do not expect eq 7 to be competitive with the alternatives.

The authors of the field measurements study[1] suggested that the unknown source of CH_3Br could be a slow or low-yield reaction involving Br atoms or BrO radicals in the boundary layer. According to their calculations, if 5% of the Br + CH_3O_2 reaction yielded $CH_3Br + O_2$ it would be enough to explain the elevated CH_3Br.[1] However, this reaction channel was subsequently shown to be uncompetitive.[7] The present study has explored another potential source of the unexplained CH_3-Br, the S_H2 displacement on CH_3I by Br. We have found this reaction also to be too slow to explain the rise in CH_3Br concentration during ozone depletion events. However, it is an unusual example of halogen substitution being competitive with H-abstraction (rate ratio 1:7). It has generally been assumed that H-abstraction predominates heavily, but this assumption breaks down for the methyl iodide case.

Conclusions

In the bimolecular reaction between Br and CH_3I, the S_H2 displacement (eq 1) is predicted to account for about 12.5% of the bimolecular products. This contradicts the usual expectation that H-abstraction predominates heavily, but is comparable to the 8.6% fraction found for the analogous, but apparently termolecular, reaction of Cl.[10] The reaction is too slow, $k_{298} = 6 \times 10^{-23}$ cm^3 molecule^{-1} s^{-1}, to explain the observed spike in the CH_3Br mixing ratio during rapid ozone depletion events in the marine boundary layer. Gas-phase reaction with BrO radicals and heterogeneous mechanisms remain to be investigated.

Note Added in Proof. The kinetic isotope effects (CH_3I vs CD_3I) are 1.08 for eq 1 and 12.6 for eq 4 (I). Thus, for CD_3I the S_H2 reaction is faster than the D-abstraction reaction (branching ratio = 1.7).

Acknowledgment. We thank Prof. Vadim Knyazev (Catholic University of America) for suggesting that we investigate eq 4.

References and Notes

(1) Wingenter, O. W.; Sive, B. C.; Blake, D. R.; Rowland, F. S.; Ridley, B. A. *Geophys. Res. Lett.* **2003**, *30*, 2160.

(2) Barrie, L. A.; Bottenheim, J. W.; Schnell, R. C.; Crutzen, P. J.; Rasmussen, R. A. *Nature* **1988**, *334*, 138−141.

(3) Bottenheim, J. W.; Barrie, L. A.; Atlas, E.; Heidt, L. E.; Niki, H.; Rasmussen, R. A.; Shepson, P. B. *J. Geophys. Res., Atmos.* **1990**, *95*, 18555−18568.

(4) Hausmann, M.; Platt, U. *J. Geophys. Res., Atmos.* **1994**, *99*, 25399−25413.

(5) Jobson, B. T.; Niki, H.; Yokouchi, Y.; Bottenheim, J.; Hopper, F.; Leaitch, R. *J. Geophys. Res., Atmos.* **1994**, *99*, 25355−25368.

(6) Ridley, B. A.; Atlas, E. L.; Montzka, D. D.; Browell, E. V.; Cantrell, C. A.; Blake, D. R.; Blake, N. J.; Cinquini, L.; Coffey, M. T.; Emmons, L. K.; Cohen, R. C.; DeYoung, R. J.; Dibb, J. E.; Eisele, F. L.; Flocke, F. M.; Fried, A.; Grahek, F. E.; Grant, W. B.; Hair, J. W.; Hannigan, J. W.; Heikes, B. J.; Lefer, B. L.; Mauldin, R. L.; Moody, J. L.; Shetter, R. E.; Snow, J. A.; Talbot, R. W.; Thornton, J. A.; Walega, J. G.; Weinheimer, A. J.; Wert, B. P.; Wimmers, A. J. *J. Geophys. Res., Atmos.* **2003**, *108*, 8356.

(7) Francisco, J. S.; Crowley, J. N. *J. Phys. Chem. A* **2006**, *110*, 3778−3784.

(8) Rasmussen, R. A.; Khalil, M. A. K.; Gunawardena, R.; Hoyt, S. D. *J. Geophys. Res. C: Oceans Atmos.* **1982**, *87*, 3086−3090.

(9) Davis, D.; Crawford, J.; Liu, S.; McKeen, S.; Bandy, A.; Thornton, D.; Rowland, F.; Blake, D. *J. Geophys. Res., Atmos.* **1996**, *101*, 2135−2147.

(10) Goliff, W. S.; Rowland, F. S. *Geophys. Res. Lett.* **1997**, *24*, 3029−3032.

(11) Ayhens, Y. V.; Nicovich, J. M.; McKee, M. L.; Wine, P. H. *J. Phys. Chem. A* **1997**, *101*, 9382−9390.

(12) Bilde, M.; Wallington, T. J. *J. Phys. Chem. A* **1998**, *102*, 1550−1555.

(13) Cotter, E. S. N.; Booth, N. J.; Canosa-Mas, C. E.; Gray, D. J.; Shallcross, D. E.; Wayne, R. P. *Phys. Chem. Chem. Phys.* **2001**, *3*, 402−408.

(14) Orlando, J. J.; Piety, C. A.; Nicovich, J. M.; McKee, M. L.; Wine, P. H. *J. Phys. Chem. A* **2005**, *109*, 6659−6675.

(15) Enami, S.; Hashimoto, S.; Kawasaki, M.; Nakano, Y.; Ishiwata, T.; Tonokura, K.; Wallington, T. J. *J. Phys. Chem. A* **2005**, *109*, 1587−1593.

(16) *Thermodynamic Properties of Individual Substances*, 4th ed.; Gurvich, L. V., Veyts, I. V., Alcock, C. B., Eds.; Hemisphere: New York, 1989.

(17) Certain commercial materials and equipment are identified in this article to specify procedures completely. In no case does such identification imply recommendation or endorsement by the National Institute of Standards and Technology, nor does it imply that the material or equipment identified is necessarily the best available for the purpose.

(18) Frisch, M. J.; Trucks, G. W.; Schlegel, H. B.; Scuseria, G. E.; Robb, M. A.; Cheeseman, J. R.; Montgomery, J. A., Jr.; Vreven, T.; Kudin, K. N.; Burant, J. C.; Millam, J. M.; Iyengar, S. S.; Tomasi, J.; Barone, V.;

Mennucci, B.; Cossi, M.; Scalmani, G.; Rega, N.; Petersson, G. A.; Nakatsuji, H.; Hada, M.; Ehara, M.; Toyota, K.; Fukuda, R.; Hasegawa, J.; Ishida, M.; Nakajima, T.; Honda, Y.; Kitao, O.; Nakai, H.; Klene, M.; Li, X.; Knox, J. E.; Hratchian, H. P.; Cross, J. B.; Adamo, C.; Jaramillo, J.; Gomperts, R.; Stratmann, R. E.; Yazyev, O.; Austin, A. J.; Cammi, R.; Pomelli, C.; Ochterski, J. W.; Ayala, P. Y.; Morokuma, K.; Voth, G. A.; Salvador, P.; Dannenberg, J. J.; Zakrzewski, V. G.; Dapprich, S.; Daniels, A. D.; Strain, M. C.; Farkas, O.; Malick, D. K.; Rabuck, A. D.; Raghavachari, K.; Foresman, J. B.; Ortiz, J. V.; Cui, Q.; Baboul, A. G.; Clifford, S.; Cioslowski, J.; Stefanov, B. B.; Liu, G.; Liashenko, A.; Piskorz, P.; Komaromi, I.; Martin, R. L.; Fox, D. J.; Keith, T.; Al-Laham, M. A.; Peng, C. Y.; Nanayakkara, A.; Challacombe, M.; Gill, P. M. W.; Johnson, B.; Chen, W.; Wong, M. W.; Gonzalez, C.; Pople, J. A. *Gaussian 03*; Gaussian, Inc.: Pittsburgh, PA, 2003.

(19) Andzelm, J.; Klobukowski, M.; Radzio-Andzelm, E. *J. Comput. Chem.* **1984**, *5*, 146−161.

(20) Glukhovtsev, M. N.; Pross, A.; McGrath, M. P.; Radom, L. *J. Chem. Phys.* **1995**, *103*, 1878−1885.

(21) Gauss, J.; Cremer, D. *Chem. Phys. Lett.* **1988**, *150*, 280−286.

(22) Pople, J. A.; Head-Gordon, M.; Raghavachari, K. *J. Chem. Phys.* **1987**, *87*, 5968−5975.

(23) McQuarrie, D. A. *Statistical Mechanics*; HarperCollins: New York, 1976.

(24) Irikura, K. K. *Thermo.pl*; National Institute of Standards and Technology: Gaithersburg, MD, 2002.

(25) Raghavachari, K.; Trucks, G. W.; Pople, J. A.; Head-Gordon, M. *Chem. Phys. Lett.* **1989**, *157*, 479−483.

(26) Raghavachari, K.; Pople, J. A.; Replogle, E. S.; Head-Gordon, M. *J. Phys. Chem.* **1990**, *94*, 5579−5586.

(27) Ralchenko, Y.; Kramida, A. E.; Reader, J.; Martin, W. C.; Musgrove, A.; Saloman, E. B.; Sansonetti, C. J.; Curry, J. J.; Kelleher, D. E.; Fuhr, J. R.; Podobedova, L.; Wiese, W. L.; Olsen, K.; Dalton, G. R.; Dragoset, R.; Jou, F.-C.; Wiersma, G. NIST Atomic Spectra Database. *NIST Standard Reference Database #78*, version 3.0.3; January 2006. National Institute of Standards and Technology. http://physics.nist.gov/asd (accessed Apr 2006).

(28) Moore, C. E. *Atomic Energy Levels*; U.S. Government Printing Office: Washington, DC, 1959; Vol. III.

(29) Visscher, L.; Eliav, E.; Kaldor, U. *J. Chem. Phys.* **2001**, *115*, 9720−9726.

(30) Jensen, H. J. A.; Saue, T.; Visscher, L.; Bakken, V.; Eliav, E.; Enevoldsen, T.; Fleig, T.; Fossgaard, O.; Helgaker, T.; Laerdahl, J.; Larsen, C. V.; Norman, P.; Olsen, J.; Pernpointner, M.; Pedersen, J. K.; Ruud, K.; Salek, P.; van Stralen, J. N. P.; Thyssen, J.; Visser, O.; Winther, T. *Dirac04*, revision 04.0; University of Southern Denmark: Odense, Denmark, 2004; http://dirac.chem.sdu.dk.

(31) Woon, D. E.; Dunning, T. H., Jr. *J. Chem. Phys.* **1995**, *103*, 4572−4585.

(32) Dunning, T. H., Jr. *J. Chem. Phys.* **1989**, *90*, 1007−1023.

(33) Dyall, K. G. *Theor. Chem. Acc.* **2006**, *115*, 441−447.

(34) Visscher, L. *Theor. Chem. Acc.* **1997**, *98*, 68−70.

(35) Werner, H.-J.; Knowles, P. J.; Lindh, R.; Manby, F. R.; Schütz, M.; Celani, P.; Korona, T.; Rauhut, G.; Amos, R. D.; Bernhardsson, A.; Berning, A.; Cooper, D. L.; Deegan, M. J. O.; Dobbyn, A. J.; Eckert, F.; Hampel, C.; Hetzer, G.; Lloyd, A. W.; McNicholas, S. J.; Meyer, W.; Mura, M. E.; Nicklass, A.; Palmieri, P.; Pitzer, R.; Schumann, U.; Stoll, H.; Stone, A. J.; Tarroni, R.; Thorsteinsson, T. *Molpro*, revision 2006.1; University College Cardiff Consultants Ltd.: Cardiff, UK, 2006.

(36) Peterson, K. A.; Figgen, D.; Goll, E.; Stoll, H.; Dolg, M. *J. Chem. Phys.* **2003**, *119*, 11113−11123.

(37) Gonzalez, C.; Schlegel, H. B. *J. Phys. Chem.* **1990**, *94*, 5523−5527.

(38) Lee, C.; Yang, W.; Parr, R. G. *Phys. Rev. B* **1988**, *37*, 785−789.

(39) Becke, A. D. *J. Chem. Phys.* **1993**, *98*, 5648−5652.

(40) Stephens, P. J.; Devlin, F. J.; Chabalowski, C. F.; Frisch, M. J. *J. Phys. Chem.* **1994**, *98*, 11623−11627.

(41) Bailleux, S.; Dréan, P.; Zelinger, Z.; Civiš, S.; Ozeki, H.; Saito, S. *J. Chem. Phys.* **2005**, *122*, 134302.

(42) Endo, Y.; Saito, S.; Hirota, E. *Can. J. Phys.* **1984**, *62*, 1347−1360.

(43) Espinosa-García, J.; Dóbé, S. *J. Phys. Chem. A* **1999**, *103*, 6387−6393.

(44) Moc, J.; Panek, J. *Chem. Phys. Lett.* **2001**, *345*, 497−504.

(45) Seetula, J. A. *Phys. Chem. Chem. Phys.* **2003**, *5*, 849−855.

(46) Li, Z. J.; Francisco, J. S. *J. Chem. Phys.* **1999**, *110*, 817−822.

(47) Li, Y. M.; Francisco, J. S. *J. Chem. Phys.* **2001**, *114*, 2879−2882.

(48) Zhang, H.; Liu, B.; Wang, L.; Li, Z.-S.; Liu, J.-Y.; Yu, X.-Y.; Sun, C.-C. *Chem. Phys. Lett.* **2006**, *420*, 12−17.

(49) Liu, Y.-J.; Ajitha, D.; Krogh, J. W.; Tarnovsky, A. N.; Lindh, R. *ChemPhysChem* **2006**, *7*, 955−963.

(50) Seetula, J. A. *Phys. Chem. Chem. Phys.* **2002**, *4*, 455−460.

(51) Taylor, B. N.; Kuyatt, C. E. *Guidelines for Evaluating and Expressing the Uncertainty of NIST Measurement Results*; NIST Technical Note 1297; National Institute of Standards and Technology: Gaithersburg, MD, 1994.

(52) Peterson, K. A.; Shepler, B. C.; Figgen, D.; Stoll, H. *J. Phys. Chem. A* **2006**, *110*, 13877−13883.

(53) Yencha, A. J.; Malins, A. E. R.; King, G. C. *Chem. Phys. Lett.* **2003**, *370*, 756−764.

(54) Seetula, J. A. *J. Chem. Soc., Faraday Trans.* **1996**, *92*, 3069−3078.

(55) Ingold, K. U.; Roberts, B. P. *Free-Radical Substitution Reactions: Bimolecular Homolytic Substitutions (S_H2 Reactions) at Saturated Multivalent Atoms*; Wiley-Interscience: New York, 1971.

(56) Bergmann, K.; Leone, S. R.; Moore, C. B. *J. Chem. Phys.* **1975**, *63*, 4161−4166.

(57) Arnold, C. C.; Neumark, D. M.; Cyr, D. M.; Johnson, M. A. *J. Phys. Chem.* **1995**, *99*, 1633−1636.

(58) Bradforth, S. E.; Weaver, A.; Arnold, D. W.; Metz, R. B.; Neumark, D. M. *J. Chem. Phys.* **1990**, *92*, 7205−7222.

(59) Imrik, K.; Kovács, G.; Fejes, I.; Szilágyi, I.; Sarzyński, D.; Dóbé, S.; Bérces, T.; Márta, F.; Espinosa-García, J. *J. Phys. Chem. A* **2006**, *110*, 6821−6832.

(60) Zhang, H.; Liu, B.; Wang, L.; Yu, X.-Y.; Li, Z.-S.; Liu, J.-Y.; Sun, C.-C. *Chem. Phys.* **2006**, *325*, 531−537.

(61) Iyer, R. S.; Rowland, F. S. *J. Phys. Chem.* **1981**, *85*, 2488−2492.

(62) Venkitachalam, T. V.; Das, P.; Bersohn, R. *J. Am. Chem. Soc.* **1983**, *105*, 7452−7453.

(63) Bartmess, J. E. In *NIST Chemistry WebBook*; Linstrom, P. J., Mallard, W. G., Eds.; National Institute of Standards and Technology: Gaithersburg, MD, June 2005. http://webbook.nist.gov/chemistry/ (accessed Feb 2007).

(64) *CRC Handbook of Chemistry and Physics*; 85th ed.; Lide, D. R., Ed.; CRC Press: Boca Raton, FL, 2004.

(65) *Constants of Diatomic Molecules (data prepared by J. W. Gallagher and R. D. Johnson, III)*; Huber, K. P., Herzberg, G., Eds.; National Institute of Standards and Technology: Gaithersburg, MD, 2001.

(66) Ruscic, B.; Boggs, J. E.; Burcat, A.; Császár, A. G.; Demaison, J.; Janoschek, R.; Martin, J. M. L.; Morton, M. L.; Rossi, M. J.; Stanton, J. F.; Szalay, P. G.; Westmoreland, P. R.; Zabel, F.; Bérces, T. *J. Phys. Chem. Ref. Data* **2005**, *34*, 573−656.

(67) Moore, C. E. *Atomic Energy Levels*; U.S. Government Printing Office: Washington, DC, 1971.

(68) Gilles, M. K.; Polak, M. L.; Lineberger, W. C. *J. Chem. Phys.* **1991**, *95*, 4723−4724.

(69) McKellar, A. R. W. *J. Mol. Spectrosc.* **1981**, *86*, 43−54.

(70) Beattie, D. A.; MacLeod, N. A.; Lawley, K. P.; Donovan, R. J. *J. Electron Spectrosc. Relat. Phenom.* **1998**, *97*, 191−196.